JOURNAL OF GEOPHYSICAL RESEARCH, VOL. 114, A09211, doi:10.1029/2008JA013729, 2009

THEMIS observations of the near-Earth plasma sheet during a substorm

C. L. Tang,[1,2] Z. Y. Li,[2] V. Angelopoulos,[3] S. B. Mende,[4] K. H. Glassmeier,[5] E. Donovan,[6] C. T. Russell,[3] and L. Lu[7]

Received 5 September 2008; revised 1 May 2009; accepted 8 May 2009; published 23 September 2009.

[1] We present observations of a substorm on 13 March 2008 by Time History of Events and Macroscale Interactions during Substorms (THEMIS) spacecraft in the near-Earth tail during the plasma sheet expansion evidenced by increase in the plasma density and temperature. The main features of the event are as follows: (1) Cross-tail current reduction or current disruption (CD) was observed in the near-Earth tail at $X \sim -8.0\ R_E$ and $Y \sim 2.0\ R_E$, marked by a sharp drop of $|B_x|$ and accompanied by sharp increases in the plasma density and temperature, manifesting a rapid expansion (recovery) of the local plasma sheet. During the course of the plasma sheet expansion, the propagation speed of the dipolarization is ~48 km/s in tailward direction and ~35 km/s in azimuthal direction. (2) In the inner edge of the plasma sheet, slow flux pileup is observed. The magnetic flux pileup is characterized by continuous enhancement of B_z and B_t and a reduction of the plasma density, pressure P_{th}, and β in the flow-braking region. The tailward moving plasma sheet expansion (CD) is also passing across the flow-braking region. In short, the dipolarization in the inner edge of the plasma sheet can be attributed to CD, while the tailward progression of dipolarization in the flow-braking region can be attributed to magnetic flux pileup. (3) A sharp decrease in the magnitude of B_x at P1 ($-13.1\ R_E$, $2.5\ R_E$, $-0.56\ R_E$) prior to the dipolarization at P5 is difficult to explain as part of the outward evolution of the CD. The rapid change in the magnetic field topology, and signatures of earthward flows and dipolarization observed at P1 prior to Pi2 onset may be caused by inward motion of flux from magnetic reconnection in the midtail ($20-30\ R_E$). Tail reconnection prior to substorm expansion can result in a sudden change of the near-Earth configuration, which may result in instabilities related to the onset of CD.

Citation: Tang, C. L., Z. Y. Li, V. Angelopoulos, S. B. Mende, K. H. Glassmeier, E. Donovan, C. T. Russell, and L. Lu (2009), THEMIS observations of the near-Earth plasma sheet during a substorm, *J. Geophys. Res.*, *114*, A09211, doi:10.1029/2008JA013729.

1. Introduction

[2] The dynamics of the near-Earth plasma sheet is an important problem in space plasma physics. The near-Earth current disruption (NECD) model suggests the following: (1) The inner magnetotail (~$8-10\ R_E$) is the source region of free energy and is where the cross-tail current density peaks prior to the expansion phase [*Kaufmann*, 1987; *Ohtani et al.*, 1992]. (2) Instabilities local to this region lead to current disruption (CD) and formation of the substorm current wedge (SCW), thus triggering expansion onset. (3) After onset, a tailward propagating rarefaction wave is generated in the CD region, initiating magnetic reconnection and bursty bulk flows (BBFs) [*Angelopoulos et al.*, 1994]. (4) Flows cause neither the CD nor the auroral breakup [*Lui et al.*, 1992; *Lyons*, 2000]. On the other hand, the near-Earth neutral line (NENL) model [*Baker et al.*, 1996; *Baumjohann*, 2002] suggests the following: (1) The BBFs originate from reconnection in the midtail, transport energy into the inner tail, and typically are stopped outside the inner region at ~$13-15\ R_E$ [*Shiokawa et al.*, 1997; *Haerendel*, 1992]. (2) Magnetic flux then piles up against this boundary, ultimately leading to a more dipolar tail configuration, and hence, to the substorm dipolarization [*Shiokawa et al.*, 1998] and expansion of the thickening plasma sheet to progressively tailward distances. (3) The pressure gradient buildup by the flow-braking causes a

[1]Institute for Space Sciences, Shandong University at Weihai, Weihai, China.
[2]School of Earth and Space Sciences, University of Science and Technology of China, Hefei, China.
[3]Department of Earth and Space Sciences, University of California, Los Angeles, California, USA.
[4]Space Sciences Laboratory, University of California, Berkeley, California, USA.
[5]TUBS, Braunschweig, Germany.
[6]Department of Physics and Astronomy, University of Calgary, Calgary, Alberta, Canada.
[7]Center for Space Science and Applied Research, Chinese Academy of Sciences, Beijing, China.

0148-0227/09/2008JA013729$09.00

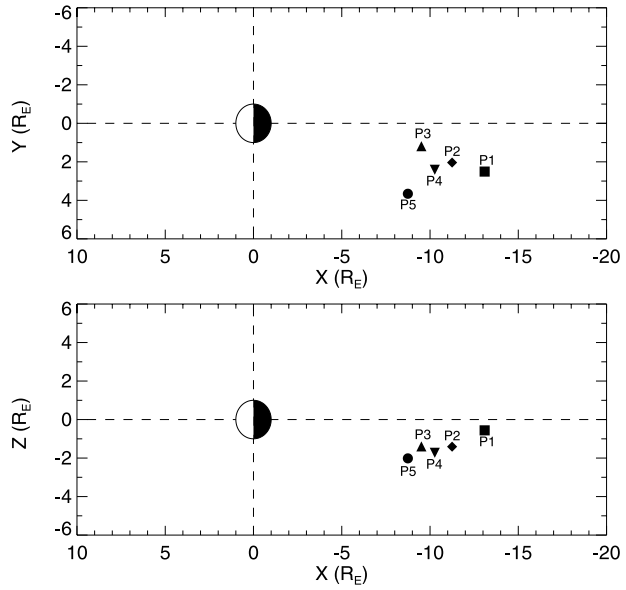

Figure 1. Projections of the THEMIS probes in the X-Y_{GSM} and X-Z_{GSM} planes at 1100 UT on 13 March 2008.

reduction and diversion of the duskward, cross-tail current, to form the SCW [*Birn et al.*, 1999].

[3] The dynamics of the near-Earth plasma sheet during substorm expansion is unclear. The Time History of Events and Macroscale Interactions during Substorms (THEMIS) mission [*Angelopoulos*, 2008; *Sibeck and Angelopoulos*, 2008] employs five identical satellites which simultaneously monitor tail phenomena to determine the substorm onset location and mechanism, and the global evolution of the substorm phenomenon. In the present study, we will present observations from THEMIS for the near-Earth plasma sheet during a substorm, and study how the current disruption evolves in longitude (or local time) and radial distance and discuss the dynamics of the near-Earth plasma sheet.

2. Overview of 13 March 2008 Event

[4] The THEMIS spacecraft configuration at 1100:00 UT is shown in Figure 1. Auroral activity was registered by the THEMIS all-sky camera array starting at ~1103:40 UT (Figure 2). Figure 3 shows the history of the integrated brightness (image totals) of all-sky images at several stations: Inuvik (INUV), Fort Yukon (FYKN), Gakona (GAKO), and White Horse (WHIT). The integrated brightness first began to increase at ~1103:00 UT at INUV (71.3 mlat, 274.7 mlon) (Figure 3a). Subsequently, the integrated brightness began to increase at ~1103:40 UT at KIAN (65.1 mlat, 253.0 mlon) (not shown; H. U. Frey, private communication, 2009), at ~1104:00 UT at FYKN (67.2 mlat, 265.7 mlon) (Figure 3b) and GAKO (63.1 mlat, 268.55 mlon) (Figure 3c). Finally, the auroral onset was at ~1104:15 UT at WHIT (63.7 mlat, 278.7 mlon) (Figure 3d). From Figure 2, the auroral activity expanded azimuthally and poleward and may, therefore, be classified as a substorm. On the basis of the start of the rapid increase of the integrated auroral intensity prior to the auroral substorm expansion, the time of substorm onset was ~1103:40 UT.

[5] Figure 4 shows the geomagnetic H component and the Pi2 pulsation of H component in the period range of 10–120 s at KIAN, FYKN, and WHIT, respectively. A negative H excursion, which is usually seen in the high-

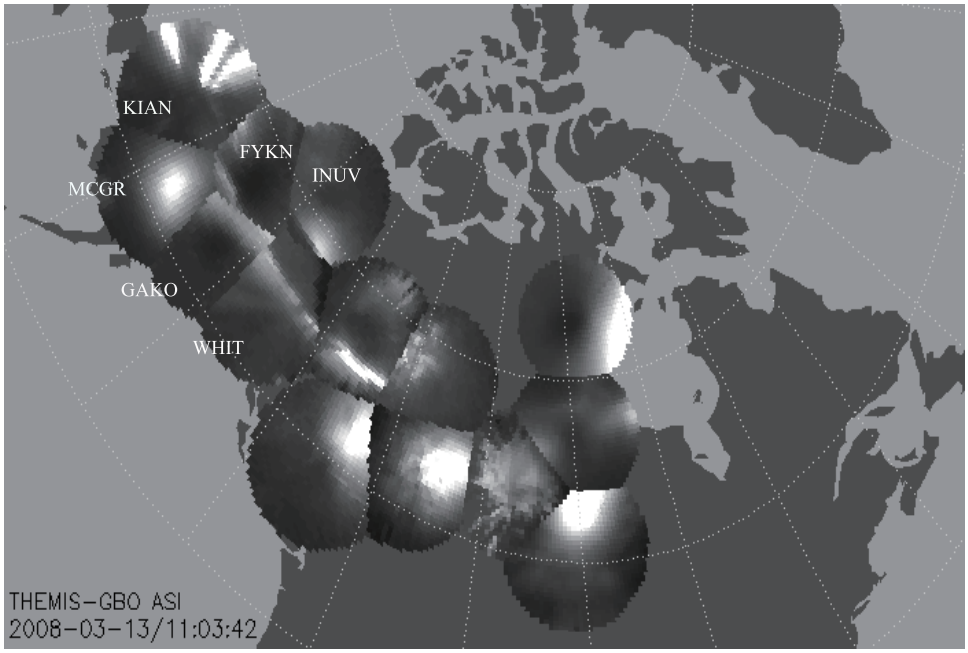

Figure 2. THEMIS all-sky camera observations around the location of substorm onset, over a continental outline. Stations used in stills are as follows: Kiana (KIAN), McGrath (MCGR), Fort Yukon (FYKN), Inuvik (INUV), Gakona (GAKO), and White Horse (WHIT). The ionospheric foot points of THEMIS probes using the T96 mapping model were located around FYKN station (not shown). GBO, ground-based observations; ASI, all-sky camera image.

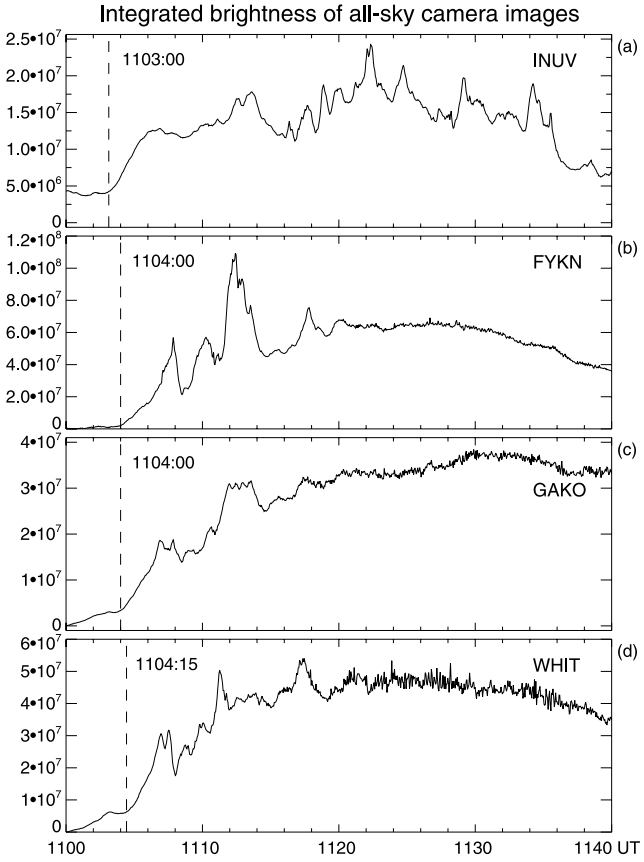

Figure 3. Integrated brightness of all-sky camera images at several stations: (a) INUV, (b) FYKN, (c) GAKO, and (d) WHIT.

latitude magnetogram, is associated with the westward auroral electrojet. The high-latitude Pi2 begins at ~1105:00 UT at KIAN (Figure 4b), almost at the same time as the negative H excursion (Figure 4a). Subsequently, a Pi2 pulsation onset was observed at ~1105:15 UT at FYKN (Figure 4d) and ~1106:00 UT at WHIT (Figure 4f). Ground Pi2 onset is typically delayed with respect to auroral breakup by ~1–2 min [*Liou et al.*, 1999], and this is consistent with our observations here; that is, auroral intensification onset (substorm onset) was at ~1103:40 UT, while high-latitude Pi2 onset was observed at 1105:00 UT (Figure 4b).

3. Observations From THEMIS

[6] P5 was located at ~(−8.7, 3.7, −2.0) R_E in GSM coordinates at 1100:00 UT. Figure 5 shows the P5 magnetic field and plasma measurements in GSM coordinates. P5 observed a slight increase in B_z at ~1107:12 UT when it was in the plasma sheet boundary layer. And, the magnetic field elevation angle θ also started to increase, which indicates the magnetic dipolarization onset at P5. At ~1109:47 UT, a sharp decrease in $|B_x|$ appeared and B_t (not shown) started to decrease, which represented a decrease of the cross-tail current. Meanwhile, the plasma density, the plasma temperature, β and the plasma pressure P_{th} all suddenly jumped up, while the magnetic pressure P_m reduced by ~0.4 nPa and the total pressure P_t reduced by ~0.2 nPa, implying a quick expansion of the plasma sheet (PS). Note that the contribution of high-energy particles from Solid State Telescope (SST) to the plasma pressure P_{th} is not considered in the present study. And, the average energy of the ions (Figure 5j) and electrons (Figures 5k and 5l) rapidly started to increase at ~1109:47 UT. This is evidence of plasma heating during the plasma sheet expansion. At ~1111:41 UT, B_z and θ started to evidently increase. During the interval, ''rebounding'' of the flows is observed, which can settle the inner magnetosphere into a new stress balance [*Slavin et al.*, 2002]. Finally, θ increased to ~36°, which shows that the tail basically remained in a dipolar shape.

[7] P1 was located at ~(−13.1, 2.5, −0.56) R_E in GSM coordinates at 1100:00 UT. Figure 6 shows the P1 magnetic field and plasma measurements. At 1105:34 UT, P1 observed a sharp decrease in $|B_x|$ when P1 entered the plasma sheet. And, β and the plasma pressure P_{th} both suddenly jumped up, while the magnetic pressure P_m reduced by ~0.4 nPa and the total pressure P_t reduced by ~0.2 nPa, which may be caused by magnetic reconnection [*Cheng*, 2004]. *Milan et al.* [2008] have shown that the magnetic pressure in the near tail decreased as closed flux was pinched off. Around 1109:00 UT, a short-lived earthward flow (V_x ~ 400 km/s) accompanied by prompt increases in B_z was detected. We referred to this phenomenon as flux pileup. While B_z, B_t and θ were increasing, plasma was possibly squeezed out, P_{th} and β then were reduced. The phenomenon was also observed by *Zhang et al.* [2007]. At ~1112:28 UT, a sharp decrease in $|B_x|$ appeared and B_t (not shown) started to decrease, which was caused by the tailward CD passing across P1. At 1114:00 UT, continuous earthward flows (V_x ~ 150 km/s) accompanied by increases in B_z were detected. These indicate that the dipolarization proceeded by ''steps'' with each flow burst event driving the B_z field to a new, higher level of dipolarization [*Slavin et al.*, 2002]. At ~1124:00 UT, the tail basically has remained in the dipolar shape. The first evidence of substorm at P1 was a gradual dipolarization at ~1103:00 UT, accompanied by equatorward convective flows ($V_z > 0$). These flows and the ensuing sharp dipolarization are difficult to reconcile with plasma sheet expansion following onset. They are likely associated with the earthward flux transport and dipolarization of reconnection prior to/during the onset of a substorm [*Angelopoulos et al.*, 2008].

[8] P2 was located at ~(−11.3, 2.0, −1.4) R_E in GSM coordinates at 1100:00 UT. Figure 7 shows the P2 magnetic field and plasma measurements. B_z and B_t (not shown) continuously started to slowly increase at ~1107:30 UT, while B_x kept nearly constant, indicating a field compression in the X direction. At ~1111:00 UT, a sharp decrease in $|B_x|$ appeared and B_t (not shown) started to decrease, which we interpret as the cross-tail current disruption reaching P2. At the same time the plasma density, the plasma temperature, β and the plasma pressure P_{th} suddenly jumped up, while the magnetic pressure P_m reduced by ~0.5 nPa and the total pressure P_t reduced by ~0.25 nPa, implying a quick expansion of the PS. The average energy of the ions (Figures 7i and 7j) and electrons (Figures 7k and 7l) rapidly started to increase at the same time. The oscillations of B_z in the Pi2 frequency range began at the same time that the dipolarization started. The Z component of the plasma flow during the interval (Figure 7f) was similar to that during the

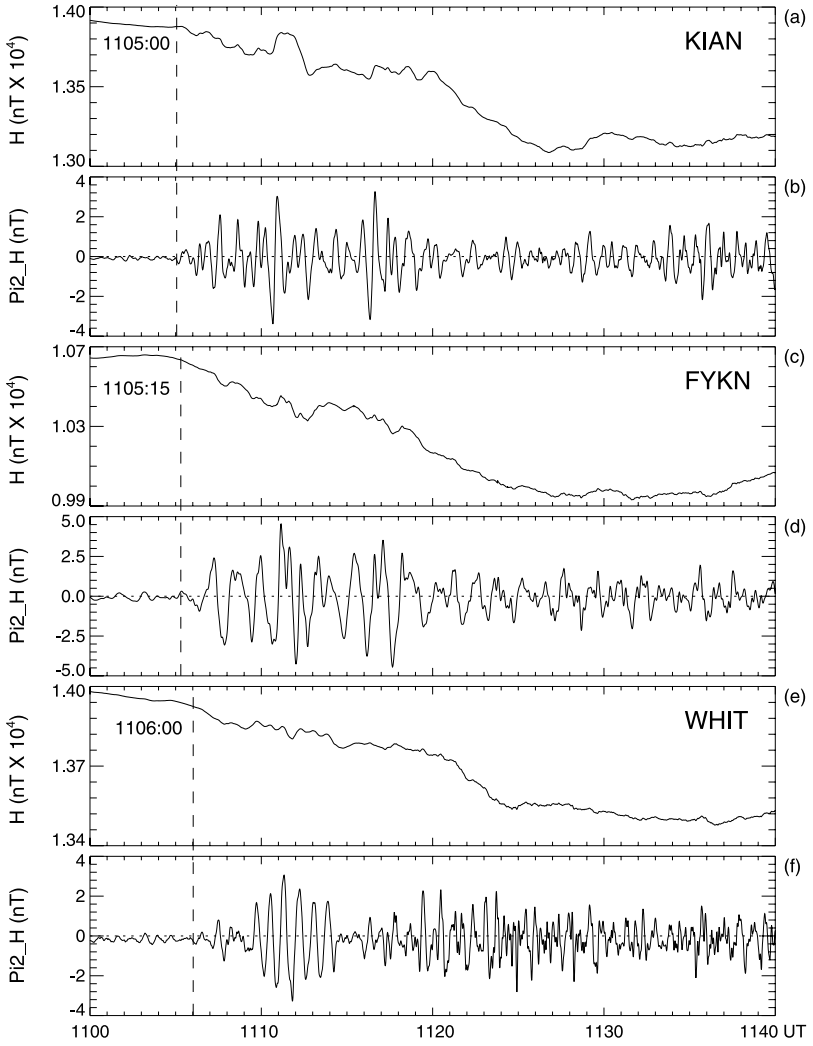

Figure 4. The geomagnetic H component and the Pi2 pulsation of H component in the period range of 10–120 s at (a, b) KIAN, (c, d) FYKN, and (e, f) WHIT. The filter includes the Pi2 band but extends to higher frequencies to reduce aliasing.

plasma sheet expansion on 27 December 2007 [*Sergeev et al.*, 2008].

[9] P3 was located at ∼(−9.5, 1.2, −1.4) R_E in GSM coordinates at 1100:00 UT. Figure 8 shows the P3 magnetic field and plasma measurements in GSM coordinates. At ∼1108:17 UT, a sharp decrease in $|B_x|$ appeared and B_t (not shown) started to decrease, which is interpreted here as the cross-tail current disruption at P3. Simultaneously, the plasma density, the plasma temperature, β and the plasma pressure P_{th} all suddenly jumped up, while the magnetic pressure P_m reduced by ∼0.6 nPa and the total pressure P_t reduced by ∼0.3 nPa, implying a quick expansion of the PS. The average energy of the ions (Figure 8j) and electrons (Figures 8k and 8l) increased rapidly at ∼1108:17 UT. P3 also observed a jump of V_x with a shorter lifetime. This type of short-lived earthward flow was commonly seen during plasma sheet expansion [*Shiokawa et al.*, 2005; *Zhang et al.*, 2007; *Cao et al.*, 2008] and is believed to be associated

Figure 5. Summary of P5 observations during the interval 1100–1140 UT on 13 March 2008: (a–c) the magnetic field measured by the Flux Gate Magnetometer (FGM) instrument; (d) the magnetic field elevation angle θ; (e) the B_z variations in the Pi2 period range (40–150 s); (f) X component (the solid line) and Z component (the dotted line) of the ion velocity measured by the Electrostatic Analyzer (ESA) instrument; (g) the magnetic pressure P_m (the solid line), plasma pressure (ions plus electrons), P_{th} (the dashed line), and the total pressure P_t (the dotted line); (h) β (the ratio of the plasma pressure to the magnetic pressure); (i, j) energy spectra of 0.005–2000 keV ions from the Solid State Telescope (SST) and ESA instruments; and (k, l) energy spectra of 0.005–2000 keV electrons from the same instruments. All energy spectrograms show omnidirectional differential energy flux (eflux) in units of eV/(cm^2 s sr eV). Magnetic field and velocity are in GSM coordinates. The vertical solid line indicates the flux pileup onset during the dipolarization process; the vertical dashed line indicates the cross-tail current disruption (CD) onset during the dipolarization process.

with the inductive electric field at substorm expansion [*Birn and Hesse*, 1998]. Finally, the thermal pressure of the plasma was about 0.5 nPa, which is near the mean thermal pressure of the ions in the plasma sheet near midnight at $X \sim -10\ R_E$ determined from the statistical analysis by *Hori et al.* [2000].

[10] P4 was located at $\sim(-10.3, 2.4, -1.7)\ R_E$ in GSM coordinates at 1100:00 UT. Figure 9 shows the P4 magnetic field and plasma measurements in GSM coordinates. B_z and B_t (not shown) started to increase at ~1107:18 UT, along with the magnetic field elevation angle θ, which indicates dipolarization onset at P4. At ~1110:00 UT, the increase in

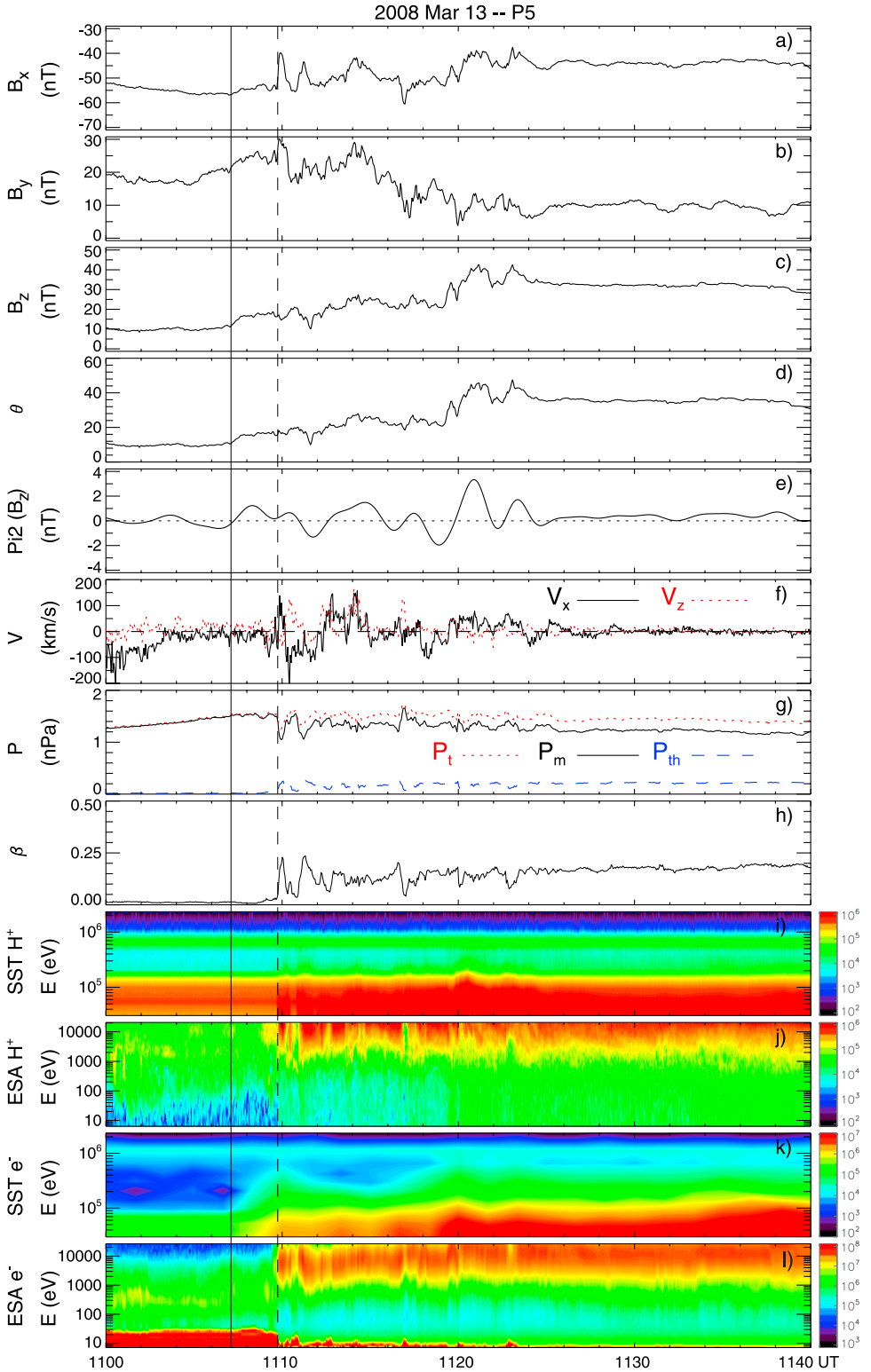

Figure 5

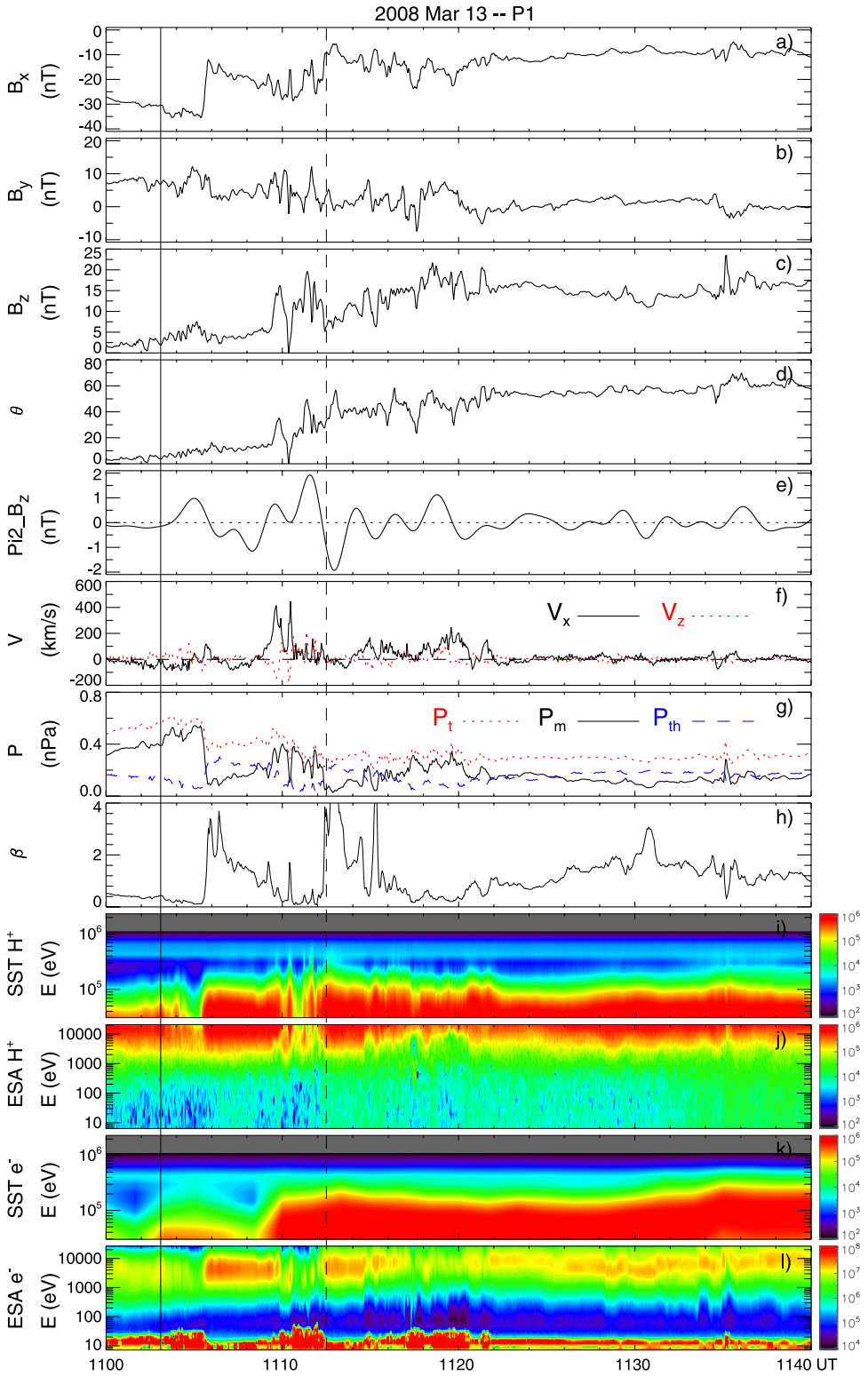

Figure 6. Summary of P1 observations during the interval 1100–1140 UT on 13 March 2008. Format is the same as that in Figure 5.

B_z accompanied by significant decrease in $|B_x|$ (and B_t), represented the cross-tail current disruption at P4 during the dipolarization process. At around the same time, the plasma density, the plasma temperature, β and the plasma pressure P_{th} all increased, while the magnetic pressure P_m and the total P_t started to decrease, implying an expansion of the PS. The average energy of the ions (Figures 9i and 9j) and electrons (Figures 9k and 9l) also stared to increase rapidly

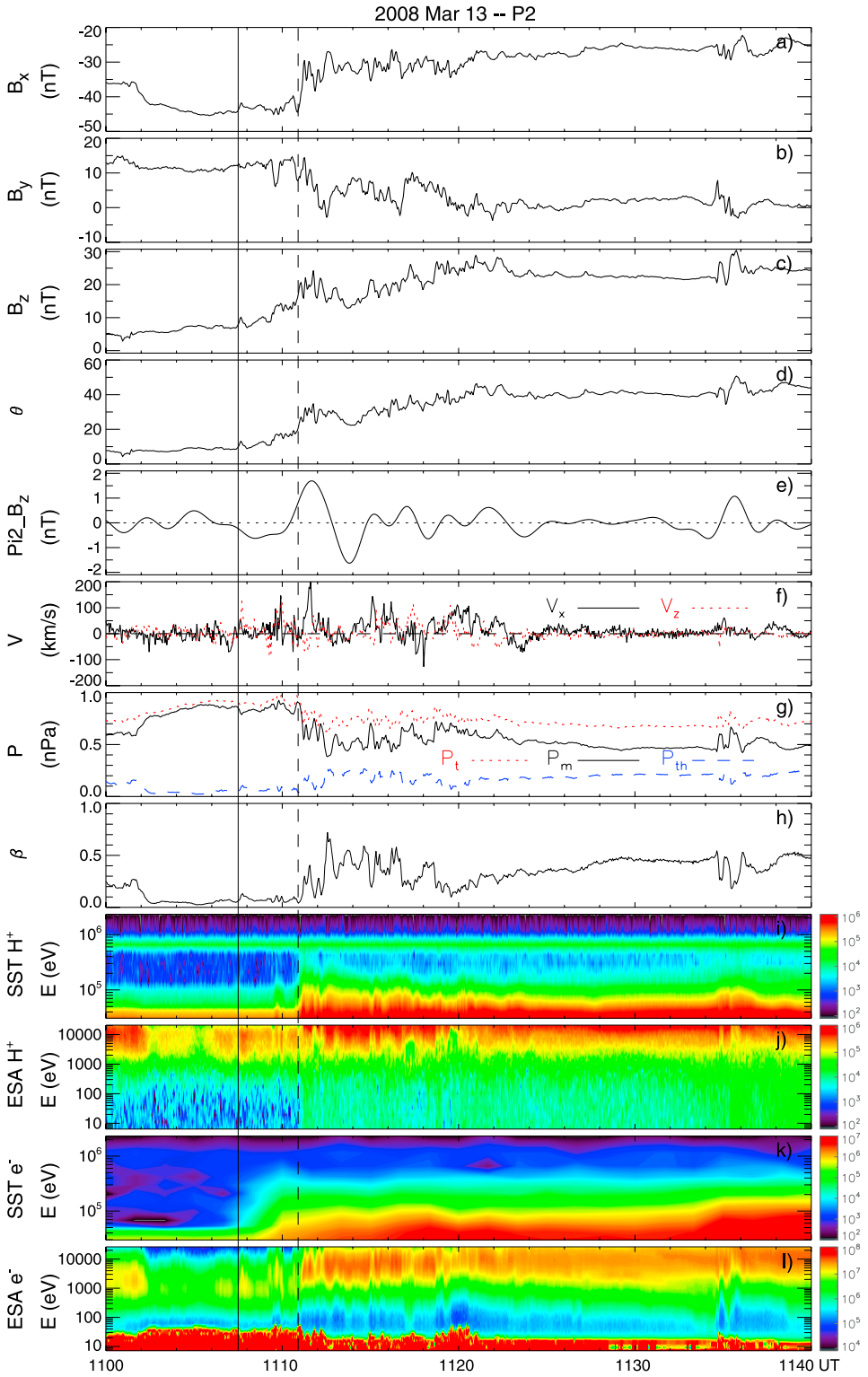

Figure 7. Summary of P2 observations during the interval 1100–1140 UT on 13 March 2008. Format is the same as that in Figure 5.

at ~1110:00 UT. Simultaneously, fluctuations in magnetic field and plasma flow were observed by P4.

4. Discussion and Summary

[11] The coordinated measurements from THEMIS multipoint observations of the near-Earth plasma sheet during a substorm on 13 March 2008 provide a wealth of information regarding the dynamics of the near-Earth plasma sheet.

4.1. Progression of the Cross-Tail Current Disruption

[12] By applying multipoint analysis techniques on Cluster and TC1 measurements, *Nakamura et al.* [2005] find that the dipolarization-related disturbances propagate main-

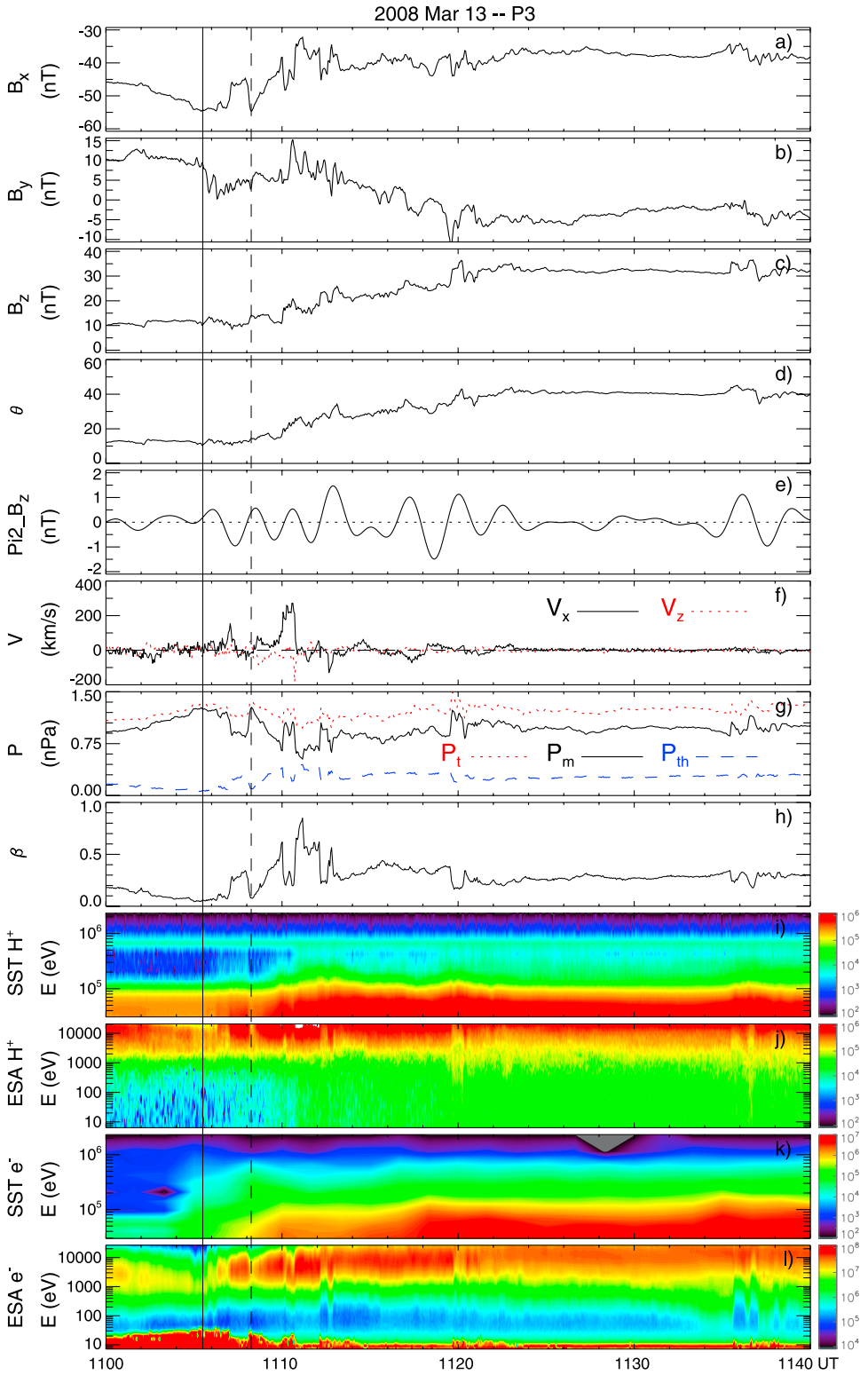

Figure 8. Summary of P3 observations during the interval 1100–1140 UT on 13 March 2008. Format is the same as that in Figure 5.

ly dawnward with a tailward component. The propagation speed, 60–190 km/s, was within the value of the previously obtained tailward propagation speeds of 35–300 km/s [*Ohtani et al.*, 1992; *Jacquey et al.*, 1993; *Baumjohann et al.*, 1999]. The THEMIS spacecraft configuration shown in Figure 1 is far better suited to the study of how the cross-tail current disruption (CD) evolves in longitude (or local time) and radial direction [*Nagai*, 1982; *Slavin et al.*, 2002]. Note that the term "CD" is used to describe the observed complex of signatures without a reference to any particular

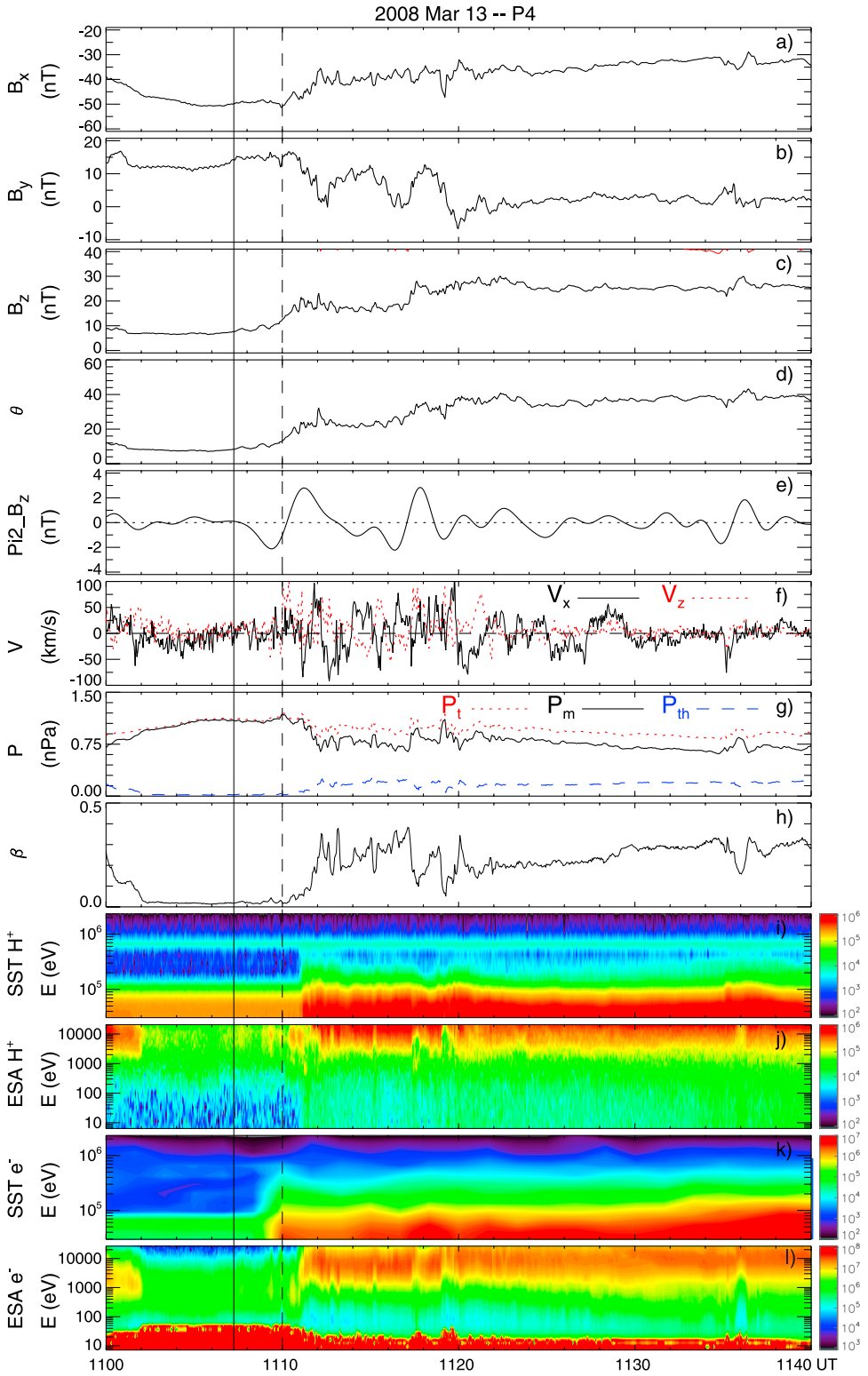

Figure 9. Summary of P4 observations during the interval 1100–1140 UT on 13 March 2008. Format is the same as that in Figure 5.

CD model. To characterize the propagation of CD more quantitatively, we compared the local propagation properties of the B_x and B_t disturbances among THEMIS probes during the dipolarization process (Figure 10). While P3 and P5 are not nearly as well aligned radially, it is of interest to note that CD is first observed at P3 at $\sim -9.5\ R_E$ and only later at $\sim -8.7\ R_E$ by P5. We interpret this as owing to azimuthal propagation delays. Combining azimuthal and radial propagation, the source region of the outward propagating dipolarization, or CD is therefore at $X \sim -8.0\ R_E$

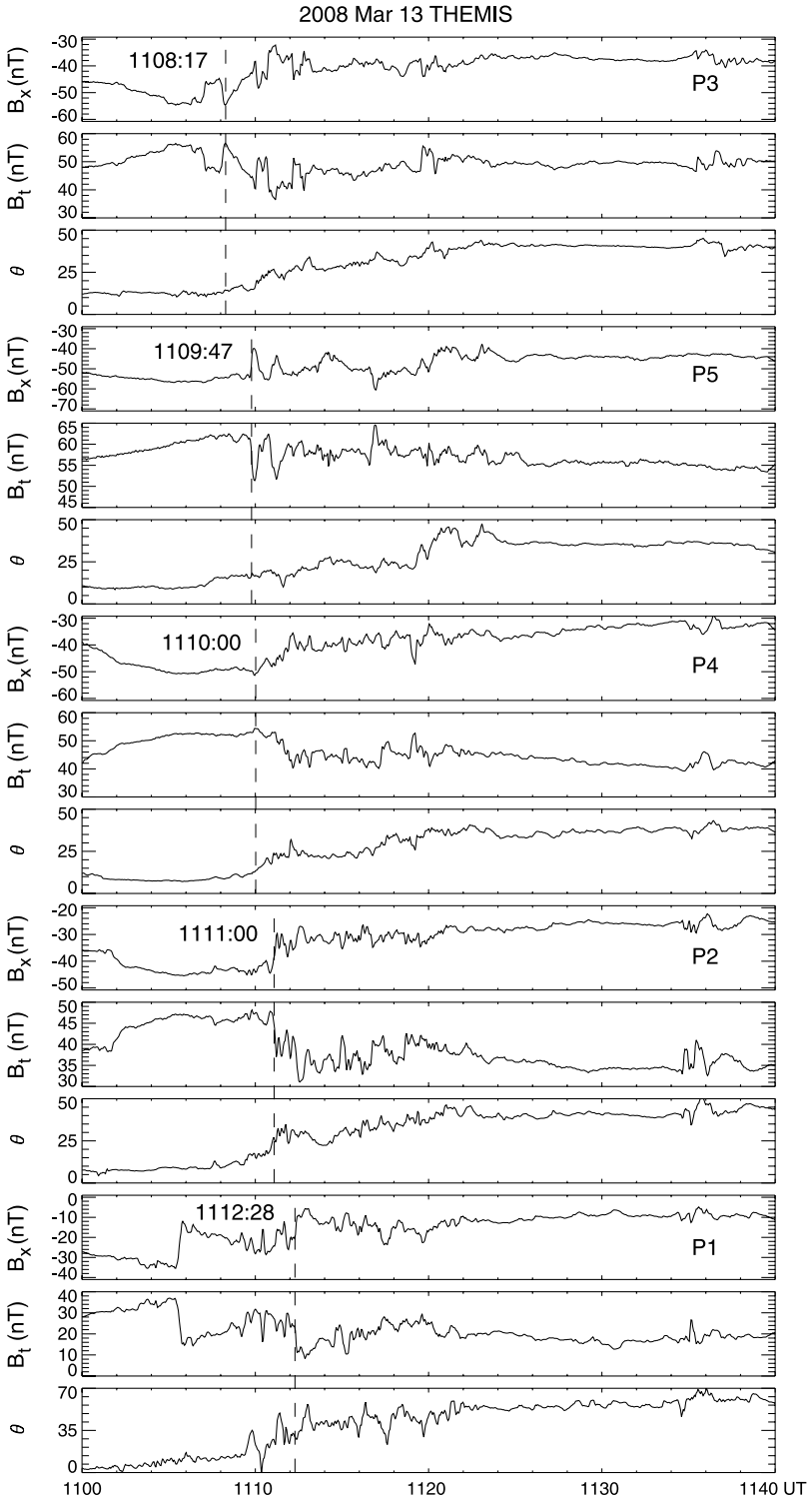

Figure 10. The progression of the cross-tail current disruption among THEMIS probes during the dipolarization process is compared using the THEMIS magnetic field measurements. From top to bottom are X component (B_x), the total magnetic field (B_t) measured by the FGM instrument, and the magnetic field elevation angle (θ) for P3, P5, P4, P2, and P1, respectively. Vertical dashed lines indicate the CD onset during the dipolarization process.

Table 1. Summary of Timing Results During the 13 March 2008, 1103:40 UT, Substorm in Order of Time Sequence

Event	Time (UT)	X_{GSM} (R_E)
Reconnection onset (P1)	1103:00 (inferred)	−13
Substorm onset	1103:40	−1
High-latitude Pi2 onset	1105:00	−1
Plasma sheet expansion at P1	1105:34	−13.1
Slow flux pileup at P5	1107:12	−8.7
Slow flux pileup at P4	1107:18	−10.3
Slow flux pileup at P2	1107:30	−11.3
Current disruption (CD) at P3	1108:17	−9.0
Earthward flow onset and flux pileup at P1	1109:00	−13.1
CD at P5	1109:47	−8.7
CD at P4	1110:00	−10.3
CD at P2	1111:00	−11.3
CD at P1	1112:28	−13.1

and $Y \sim 2.0\ R_E$. The progression speed of the expanding dipolarization/CD is ∼48 km/s in tailward direction and ∼35 km/s in azimuthal direction.

4.2. Tailward Progression of the Dipolarization

[13] The tailward progression of dipolarization at multiple activity sites is a shared feature of the NECD [*Jacquey et al.*, 1991, 1993; *Perraut et al.*, 2003; *Lui*, 1996, 2004] and NENL [*Baumjohann et al.*, 1999] models. In the NECD model, the magnetic field dipolarization is related with cross-tail current reduction (CD) and localized particle energization [*Lui*, 1996]. CD initiates a tailward propagating rarefaction wave that triggers reconnection and BBFs as the wave reaches the midtail [*Chao et al.*, 1977; *Lui*, 1991]. In the NENL model, the BBFs originate from reconnection in the midtail, transport energy into the inner tail, and typically are stopped outside the inner region at ∼−13 to −15 R_E [*Shiokawa et al.*, 1997]. Magnetic flux then piles up against this boundary, ultimately leading to a more dipolar tail configuration, and hence, to the substorm dipolarization [*Shiokawa et al.*, 1998; *Birn et al.*, 1999]. It is suggested that once the tailward moving dipolarization front arrives at the reconnection site, the near-Earth neutral line disappears [*Baumjohann et al.*, 1999]. *Baumjohann et al.* [1999] consider this feature as the classical signature of the beginning of the recovery phase.

[14] In this study, the tailward progression of cross-tail current disruption and flux pileup are observed during the dipolarization process. The tailward propagation of the dipolarization/CD in the inner edge of the plasma sheet was successively observed by P3, P5, P4, and P2 (Figure 10), which is marked by a sharp drop of $|B_x|$ and sudden jumps of the plasma density and temperature, manifesting a rapid expansion of the local plasma sheet. *Shiokawa et al.* [1997] have shown that in most cases the BBF was braking and piled up flux tailward of $X \sim -13$ to $-15\ R_E$. In the inner edge of the plasma sheet, the BBFs are generally observed less frequently. However, in our case, slow flux pileup is successively observed at ∼1107:12 UT at P5, at ∼1107:18 UT at P4 and at ∼1107:30 UT at P2. Flux pileup is seen at the flow-braking region (−13.1 R_E) by P1 at ∼1109:00 UT, which is characterized by enhancements of B_z and B_t with the trend of reduction of the plasma density, the plasma pressure P_{th} and β. During the interval of flux pileup, the tailward expansion of the dipolarization/CD was also observed at the P1 location (Figure 10). This shows that at the P1 location there are two distinct processes: It is likely that convection, evidenced by equatorward flows and dipolarization already from 1103 UT and plasma sheet expansion at 1105 UT, resulting in an earthward motion of compressed magnetic field and fast-mode waves propagating inward that yield compression of B_z and the related oscillations in Pi2 frequency range. On the other hand, as the CD originates around P3 ($X \sim -8.0\ R_E$ and $Y \sim 2.0\ R_E$) it is possible that the dipolarization front associated with the interaction of the inward flows and the strong dipole field creates a distinct current disruption process. As the plasma sheet expands, the CD moves tailward. Subsequently, P1 at the flow-braking region also observes a tailward propagating CD and high-speed flows at 1109 UT which completely subside by 1112 UT at P1. In short, the dipolarization in the inner edge of the plasma sheet may be attributed to a distinct CD process driven by the initial flux transport seen at P1 early in the substorm process, while the tailward progression of dipolarization in the flow-braking region may be attributed to magnetic flux pileup.

4.3. Substorm Spatial and Temporal Evolution

[15] The THEMIS observations of the 13 March 2008 substorm in this study are summarized in Table 1. Figure 6a shows the sharp decrease in $|B_x|$ at 1105:34 UT at P1. The rapid change of the magnetic field topology may be caused by magnetic reconnection in midtail (20−30 R_E). If we were to interpret the sharp change in B_x at P1 as owing to CD, it would be difficult to explain the travel of CD as discussed earlier. The high-latitude Pi2 begins at ∼1105:00 UT at KIAN (Figure 4b), which may signify the arrival of the field-aligned current pulse generated by the reconnection flows in the tail [*Kepko et al.*, 2004]. These are consistent with the observations of inward flow Vz > 0 and dipolarization at P1 two minutes earlier. The two observations allow us to infer the formation of the NENL at ∼1103:00 UT. The substorm event may be directly triggered by tail reconnection [*Angelopoulos et al.*, 2008]. The slow flux pileup is successively observed at ∼1107:12 UT at P5, at ∼1107:18 UT at P4 and at ∼1107:30 UT at P2. Around 1109:00 UT, a short-lived earthward flow ($V_x \sim 400$ km/s) accompanied by prompt increases in B_z is detected at P1. *Pu et al.* [1999, 2001] suggested that the interaction between the flow-braking region and the inner edge of the plasma sheet, and the resultant flow braking, might yield favorable conditions for instabilities to grow near the inner edge of the plasma sheet, eventually leading to dipolarization at substorm onset. Recently, it was shown by modeling that an Earthward BBF may trigger nonlinear ballooning instability at the inner edge of the plasma sheet [*Voronkov*, 2005]. The model predicts a jump-like increase of the plasma pressure, collapse-like dynamics of the magnetic field (a rapid reduction of the cross-tail current) in tens of seconds, with subsequent tailward expansion of the unstable region. In our case, P3 first observed a sharp decrease in $|B_x|$ at ∼1108:17 UT. Subsequently, the tailward propagating CD was successively observed by P5, P4, P2, and eventually at P1 (Figure 10). Our observations also show that before substorm expansion onset, tail reconnection may lead to a sudden change of the near-Earth configuration, which may lead to instabilities in this region then trigger sharp dipolarization/CD.

[16] We have presented observations of a substorm on 13 March 2008 by THEMIS (Table 1). The major results for the substorm event can be summarized as follows:

[17] 1. The cross-tail current reduction or disruption (CD) initiates in the near-Earth tail at $X \sim -8.0\ R_E$ and $Y \sim 2.0\ R_E$, which is marked by a sharp drop of $|B_x|$ with sharp increases in the plasma density and temperature, manifesting a rapid expansion of the local plasma sheet. During the course of the plasma sheet expansion, the progression speed of CD is ~48 km/s in tailward direction and ~35 km/s in azimuthal direction.

[18] 2. In the inner edge of the plasma sheet, slow magnetic flux pileup is observed. It is characterized by continuous enhancement of B_z and B_t with a trend of reduction in the plasma density, the plasma pressure P_{th} and β in the flow-braking region. The tailward moving CD is also passing across the flow brake region. The dipolarization in the inner edge of the plasma sheet may be attributed to a distinct CD process, while the tailward progression of dipolarization in the flow brake region may mainly be attributed to magnetic flux pileup.

[19] 3. The equatorward flows and initial dipolarization at P1 ($-13.1\ R_E$, $2.5\ R_E$, $-0.56\ R_E$) at 1103 UT, followed by a sharp decrease in $|B_x|$, all prior to the flux pileup and fast earthward flows at 1109 UT, are difficult to explain as part of the evolution of the CD. The rapid change in the magnetic field topology may be caused by magnetic reconnection in midtail ($20-30\ R_E$). Tail reconnection before substorm expansion onset can lead to a sudden change of the near-Earth configuration, which may lead to instabilities in this region then trigger the CD.

[20] **Acknowledgments.** The study was supported by the Chinese National Natural Science Foundation Committee grants 40825014, 40890162, and 40774094. We acknowledge I. Mann for use of the GMAG data and the CSA for support of the CARISMA network. The work by V. Angelopoulos, S. Mende, and C. T. Russell was supported by NASA contract NAS5–02099. The FGM team under the lead of the Technical University of Braunschweig is financially supported through the German Ministry for Economy and Technology and the German Center for Aviation and Space (DLR) under contract 50 OC 0302. We are grateful to H. U. Frey for providing the ASIs data. We thank C. W. Carlson and J. P. McFadden for the use of the THEMIS/ESA data and appreciate useful discussions with J. P. McFadden and X. Cao.

[21] Zuyin Pu thanks the reviewers for their assistance in evaluating this paper.

References

Angelopoulos, V. (2008), The THEMIS mission, *Space Sci. Rev.*, *141*, 5–34, doi:10.1007/s11214-008-9336-1.

Angelopoulos, V., C. F. Kennel, F. V. Coroniti, R. Pellat, M. G. Kivelson, R. J. Walker, C. T. Russell, W. Baumjohann, W. C. Feldman, and J. T. Gosling (1994), Statistical characteristics of bursty bulk flow Events, *J. Geophys. Res.*, *99*(A11), 21,257–21,280.

Angelopoulos, V., et al. (2008), Tail reconnection triggering substorm onset, *Science*, *321*, 931–935, doi:10.1126/science.1160495.

Baker, D. N., T. I. Pulkkinen, V. Angelopoulos, W. Baumjohann, and R. L. McPherron (1996), Neutral line model of substorms: Past result and present view, *J. Geophys. Res.*, *101*(A6), 12,975–13,010, doi:10.1029/95JA03753.

Baumjohann, W. (2002), Modes of convection in the magnetotail, *Phys. Plasmas*, *9*(9), 3665–3667, doi:10.1063/1.1499116.

Baumjohann, W., M. Hesse, S. Kokubun, T. Mukai, T. Nagai, and A. A. Petrukovich (1999), Substorm dipolarization and recovery, *J. Geophys. Res.*, *104*, 24,995–25,000, doi:10.1029/1999JA900282.

Birn, J., and M. Hesse (1998), Substorm effects in MHD and test particle simulations of magnetotail dynamics, in *Proceedings of International Conference on Substorms-4, Lake Hamana, Japan, March 9–13, 1998*, edited by S. Kokubun and Y. Kamide, pp. 159–164, Kluwer Acad., Boston.

Birn, J., M. Hesse, G. Haerendel, W. Baumjohann, and K. Shiokawa (1999), Flow braking and the substorm current wedge, *J. Geophys. Res.*, *104*, 19,895–19,904, doi:10.1029/1999JA900173.

Cao, X., et al. (2008), Multispacecraft and ground-based observations of substorm timing and activations: Two case studies, *J. Geophys. Res.*, *113*, A07S25, doi:10.1029/2007JA012761.

Chao, J. K., J. R. Kan, A. T. Y. Lui, and S.-I. Akasofu (1977), A model for thinning of the plasma sheet, *Planet. Space Sci.*, *25*, 703–710, doi:10.1016/0032-0633(77)90122-2.

Cheng, C. Z. (2004), Physics of substorm growth phase, onset, and dipolarization, *Space Sci. Rev.*, *113*, 207–270, doi:10.1023/B:SPAC.0000042943.59976.0e.

Haerendel, G. (1992), Disruption, ballooning or auroral avalanche: On the cause of substorms, in *Proceedings of the First International Conference on Substorms (ICS-1). Kiruna, Sweden, 23–27 March 1992*, *ESA SP-335*, pp. 417–420, Eur. Space Agency, Paris.

Hori, T., K. Maezawa, Y. Saito, and T. Mukai (2000), Average profile of ion flow and convection electric field in the near-Earth plasma sheet, *Geophys. Res. Lett.*, *27*, 1623–1626, doi:10.1029/1999GL003737.

Jacquey, C. J., A. Sauvaud, and J. Dandouras (1991), Location and propagation of the magnetotail current disruption during substorm onset: Analysis and simulation of an ISEE multi-onset event, *Geophys. Res. Lett.*, *18*, 389–392, doi:10.1029/90GL02789.

Jacquey, C., J. A. Sauvaud, I. Dandouras, and A. Korth (1993), Tailward propagating cross-tail current disruption and dynamics of near-Earth tail: A multi-point measurement analysis, *Geophys. Res. Lett.*, *20*, 983–986, doi:10.1029/93GL00072.

Kaufmann, R. L. (1987), Substorm currents: Growth phase and onset, *J. Geophys. Res.*, *92*, 7471–7486, doi:10.1029/JA092iA07p07471.

Kepko, L., M. G. Kivelson, and R. L. McPherron (2004), Relative timing of substorm onset phenomena, *J. Geophys. Res.*, *109*, A04203, doi:10.1029/2003JA010285.

Liou, K., C.-I. Meng, T. Lui, P. Newell, M. Brittnacher, G. Parks, G. Reeves, R. Anderson, and K. Yumoto (1999), On relative timing in substorm onset signatures, *J. Geophys. Res.*, *104*, 22,807–22,817, doi:10.1029/1999JA900206.

Lui, A. T. Y. (1991), Extended consideration of a synthesis model for magnetospheric substorms, in *Magnetospheric Substorms*, edited by J. R. Kan et al., 43 pp., AGU, Washington, D. C.

Lui, A. T. Y. (1996), Current disruption in the Earth's magnetosphere: Observations and models, *J. Geophys. Res.*, *101*, 13,067–13,088, doi:10.1029/96JA00079.

Lui, A. T. Y. (2004), Potential plasma instabilities for substorm expansion onsets, *Space Sci. Rev.*, *113*, 127–206, doi:10.1023/B:SPAC.0000042942.00362.4e.

Lui, A. T. Y., R. E. Lopez, B. J. Anderson, K. Takahashi, L. J. Zanetti, R. W. McEntire, T. A. Potemra, D. M. Klumpar, E. M. Greene, and R. Strangeway (1992), Current disruptions in the near-Earth neutral sheet region, *J. Geophys. Res.*, *97*, 1461–1480, doi:10.1029/91JA02401.

Lyons, L. R. (2000), Determination of relative timing of near-Earth substorm onset and tail reconnection, in *Proceedings of the Fifth International Conference on Substorms ICS-5*, *Eur. Space Agency Spec. Publ.*, *ESA SP-443*, 255–258.

Milan, S. E., P. D. Boakes, and B. Hubert (2008), Response of the expanding/contracting polar cap to weak and strong solar wind driving: Implications for substorm onset, *J. Geophys. Res.*, *113*, A09215, doi:10.1029/2008JA013340.

Nagai, T. (1982), Observed magnetic substorm signatures at synchronous altitude, *J. Geophys. Res.*, *87*, 4405–4417, doi:10.1029/JA087iA06p04405.

Nakamura, R., et al. (2005), Cluster and Double Star observations of dipolarization, *Ann. Geophys.*, *23*, 2915–2920.

Ohtani, S.-I., et al. (1992), Initial signatures of magnetic field and energetic particle fluxes at tail reconfiguration: Explosive growth phase, *J. Geophys. Res.*, *97*, 19,311–19,324, doi:10.1029/92JA01832.

Perraut, S., O. L. Contel, A. Roux, G. Parks, D. Chua, M. Hosshino, T. Mukai, and T. Nagai (2003), Substorm expansion phase: Observations from Geotail, Polar and IMAGE network, *J. Geophys. Res.*, *108*(A4), 1159, doi:10.1029/2002JA009376.

Pu, Z. Y., et al. (1999), Ballooning instability in the presence of a plasma flow: A synthesis of tail reconnection and current disruption models for the initiation of substorms, *J. Geophys. Res.*, *104*, 10,235–10,248, doi:10.1029/1998JA900104.

Pu, Z. Y., A. Korth, Z. X. Chen, Z. X. Liu, S. Y. Fu, G. Zong, M. H. Hong, and X. M. Wang (2001), A global synthesis model of dipolarization at substorm expansion onset, *J. Atmos. Sol. Terr. Phys.*, *63*, 671–681, doi:10.1016/S1364-6826(00)00183-8.

Sergeev, V. A., S. V. Apatenkov, V. Angelopoulos, J. P. McFadden, D. Larson, J. W. Bonnell, M. Kuznetsova, N. Partamies, and F. Honary (2008), Simultaneous THEMIS observations in the near-tail portion of

the inner and outer plasma sheet flux tubes at substorm onset, *J. Geophys. Res.*, *113*, A00C02, doi:10.1029/2008JA013527.

Shiokawa, K., W. Baumjohann, and G. Haerendel (1997), Braking of high-speed flows in the near-Earth tail, *Geophys. Res. Lett.*, *24*, 1179–1182, doi:10.1029/97GL01062.

Shiokawa, K., et al. (1998), High-speed ion flow, substorm current wedge, and multiple Pi 2 pulsations, *J. Geophys. Res.*, *103*, 4491–4507, doi:10.1029/97JA01680.

Shiokawa, K., I. Shinohara, T. Mukai, H. Hayakawa, and C. Z. Cheng (2005), Magnetic field fluctuations during substorm-associated dipolarizations in the nightside plasma sheet around $X = -10$ R_E, *J. Geophys. Res.*, *110*, A05212, doi:10.1029/2004JA010378.

Sibeck, D. G., and V. Angelopoulos (2008), THEMIS science objectives and mission phases, *Space Sci. Rev.*, *141*, 35–39, doi:10.1007/s11214-008-9393-5.

Slavin, J. A., et al. (2002), Simultaneous observations of earthward flow bursts and plasmoid ejection during magnetospheric substorms, *J. Geophys. Res.*, *107*(A7), 1106, doi:10.1029/2000JA003501.

Voronkov, I. O. (2005), Near-Earth breakup triggered by the earthward traveling burst flow, *Geophys. Res. Lett.*, *32*, L13107, doi:10.1029/2005GL022983.

Zhang, H., et al. (2007), TC-1 observations of flux pileup and dipolarization-associated expansion in the near-Earth magnetotail during substorms, *Geophys. Res. Lett.*, *34*, L03104, doi:10.1029/2006GL028326.

V. Angelopoulos and C. T. Russell, Department of Earth and Space Sciences, University of California, Los Angeles, CA 90095, USA.

E. Donovan, Department of Physics and Astronomy, University of Calgary, Calgary, AB, Canada T2N 1N4.

K. H. Glassmeier, TUBS, Braunschweig, D-38106 Germany.

Z. Y. Li, School of Earth and Space Sciences, University of Science and Technology of China, Hefei, Anhui 230026, China.

L. Lu, Center for Space Science and Applied Research, Chinese Academy of Sciences, Beijing 100080, China.

S. B. Mende, Space Sciences Laboratory, University of California, Berkeley, CA 94720, USA.

C. L. Tang (corresponding author), Institute for Space Sciences, Shandong University at Weihai, Weihai, Shandong 264209, China. (tcl@mail.ustc.edu.cn)